Proceedings of the 2003 IEEE
International Conference on Robotics & Automation
Taipei, Taiwan, September 14-19, 2003

CVT Control of an Omnidirectional Mobile Robot with Steerable Omnidirectional Wheels for Energy Efficient Drive

Kyung-Seok Byun

Mechatronics Center, Samsung Electronics
416, Maetan-dong, Paldal-gu, Suwon City, 442-742, Korea
ks1.byun@samsung.com

Jae-Bok Song

Dept. of Mechanical Eng., Korea University
5, Anam-dong Sungbuk-gu, Seoul, 136-701, Korea
jbsong@korea.ac.kr

Abstract **– In a previous research, a new class of an omnidirectional mobile robot was proposed. Since it has synchronously steerable omnidirectional wheels, it is called an omnidirectional mobile robot with steerable omnidirectional wheels (OMR-SOW). It has 3 DOFs in motion and one DOF in steering. One steering DOF can function as a continuously variable transmission (CVT). CVT of the OMR-SOW increases the range of velocity ratio from the wheel velocities to robot velocity, which may improve performance of a mobile robot. In this paper, kinematics and dynamics of this robot will be analyzed. A control algorithm for CVT mounted on the OMR-SOW, which considers motor efficiency in its operation, is discussed in detail. Various tests have been conducted to demonstrate validity and feasibility of the proposed mechanism and the steering algorithm. Experimental results show the OMR-SOW can be driven more efficiently with the proposed steering algorithm and a CVT mechanism.**

I. INTRODUTION

Omnidirectional mobile robots are capable of moving in an arbitrary direction without changing the direction of wheels, because they can achieve 3 DOF motion on a 2-dimensional plane. Various types of omnidirectional mobile robots have been proposed so far; universal wheels [1, 2], ball wheels [3], off-centered wheels [4] are popular among them.

In a previous research [5], an omnidirectional mobile robot with steerable omnidirectional wheels (OMR-SOW) shown in Fig. 1 was proposed to improve CVT performance. The OMR-SOW is an omnidirectional mobile robot with 3 DOF motion and 1 DOF in steering. The steering DOF can be achieved by synchronously steerable omnidirectional wheels. While the variable footprint mechanism (VFM) proposed by Wada and Asada [9], has a common steering axis for all four wheels, the OMR-SOW has an independent steering axis for each wheel. Therefore, the OMR-SOW possesses a wider range of velocity ratio without stability degradation.

In this paper, a control algorithm for CVT of the OMR-SOW is discussed. The CVT of the OMR-SOW provides possibility of energy efficient drive. If the CVT is not properly controlled, however, energy efficiency capability can be deteriorated. Hence, a proper control algorithm is essential to energy efficient drive. The CVT control algorithms for automobiles have been developed by many research groups, [7,8] but the CVT control of OMR-SOW is different from those algorithms. While the automobile CVT is related to one actuator (i.e., an engine), the CVT of OMR-SOW is related to all four motors. In this research, a simple and effective algorithm for control of CVT considering efficiency of a motor drive is suggested and verified by various experiments.

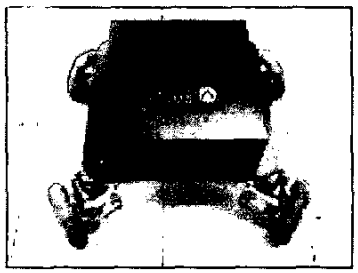

Fig. 1 Photo of OMR-SOW

The remainder of this paper is organized as follows. In Section 2, kinematics and dynamics of the OMR-SOW are introduced. Section 3 explains motion control of the robot, and discusses the CVT control algorithm. Section 4 shows experimental results and Section 5 concludes the research results.

II. OMR-SOW

A. Structure of OMR-SOW

The coordinate systems for the OMR-SOW are illustrated in Fig. 2. Notice that the four wheel modules can rotate about each pivot point C_1, .., C_4 located at the corners of the robot body, but they are constrained to have a synchronized steering motion of 1 DOF by the synchronous mechanism comprising the connecting links and linear guide [5]. In Fig. 2, the steering angle ϕ is defined as the angle from the zero position in which the lines connecting the centers of diagonally opposed wheels coincide with the diagonal lines (i.e., C_1C_3 or C_2C_4) of the robot body. Figure 3 shows various wheel arrangements.

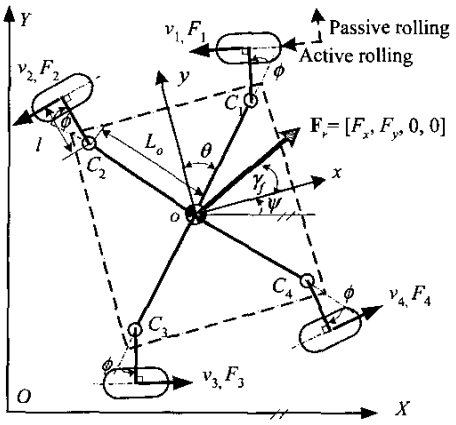

Fig. 2 Coordinate systems for omnidirectional mobile robot under consideration

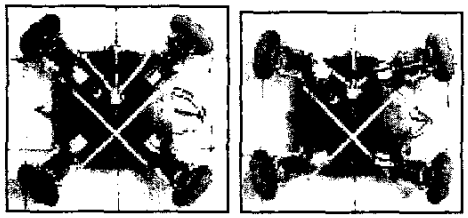

(a) $\phi = 0^o$ (b) $\phi = -30^o$

Fig. 3 Various wheel arrangements of OMR-SOW.

This robot contains the wheel module comprising the four omnidirectional wheels connected to individual motors, a variable wheel arrangement mechanism, and a square platform whose side is 500mm [5]. The omnidirectional wheels used in the robot are called the *continuous alternate wheel* developed in our laboratory, where inner and outer rollers are arranged continuously, thus resulting in no gap between the rollers [9]. These wheels are connected to the DC motors through timing belts. Wheel suspension systems are required to ensure that the wheels are in contact with the ground at all times. This suspension can also absorb the shock transmitted to the wheels.

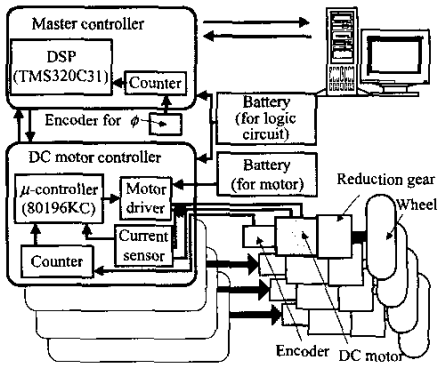

Fig. 4 Control systems for OMR-SOW

Fig. 4 illustrates the control systems for the mobile robot. DSP (TMS320C31) is used as a master controller, while the microcontroller 80196KC is employed as a motor controller. The master controller plans the robot trajectory and gives the commands to the motor drives where motor control is performed.

B. Kinematic Analysis

As shown in Fig. 2, the frame *O-XY* is assigned as a reference frame for the robot motion in the plane and the moving frame *o-xy* is attached to the robot center. On the other hand, the angle θ between the *y*-axis and the diagonal line of the robot platform depends on the shape of a platform. (i.e., $\theta = 45^\circ$ for the square platform)

The relationship between the wheel velocity vector $\mathbf{V}_w$ and the vehicle velocity vector $\mathbf{V}_r$ can be expressed from the geometry in Fig. 2 by

$$\mathbf{V}_w = \mathbf{J}^{-1}\mathbf{V}_r \quad \text{or} \quad \mathbf{V}_r = \mathbf{J}\,\mathbf{V}_w \tag{1}$$

where $\mathbf{V}_w = [v_1 \;\; v_2 \;\; v_3 \;\; v_4]^T, \mathbf{V}_r = [v_x \;\; v_y \;\; \dot{\psi} \;\; \dot{\phi}]^T$,

$$\mathbf{J} = \frac{1}{4}\begin{bmatrix} -1/C & -1/C & 1/C & 1/C \\ 1/S & -1/S & -1/S & 1/S \\ 1/L & 1/L & 1/L & 1/L \\ 1/l & -1/l & 1/l & -1/l \end{bmatrix}, \text{where } \begin{cases} C = \cos(\theta - \phi) \\ S = \sin(\theta - \phi) \\ L = L_o \cos\phi + l \end{cases}$$

Here, v_1, v_2, v_3, and v_4 are the wheel velocities in the active direction, v_x and v_y are the translational velocities of the robot center, $\dot{\psi}$ is the angular velocity about the robot center, and $\dot{\phi}$ is the derivative of the steering angle, respectively. **J** is the Jacobian matrix relating the wheel velocity vector to the robot velocity vector. The Jacobian is invertible, provided $0 < \theta - \phi < 90^o$ because $C \neq 0$ and $S \neq 0$. It follows from Eq. (1) that the robot velocity and the steering velocity of a variable wheel arrangement mechanism can be completely determined by control of four independent motors driving each wheel.

C. Dynamic Analysis

The dynamic model of the robot should be obtained for use in the CVT control algorithm. Consider the dynamic model of a robot shown in Fig. 1. The robot motion on the fixed coordinate system XY is described by

$$\mathbf{M}_r \dot{\mathbf{V}}_R = \mathbf{F}_R \tag{2}$$

where

$$\mathbf{M}_r = \begin{bmatrix} M & 0 & 0 & 0 \\ 0 & M & 0 & 0 \\ 0 & 0 & I_z & 0 \\ 0 & 0 & 0 & I_\phi \end{bmatrix}, \mathbf{V}_R = \begin{bmatrix} v_X \\ v_Y \\ \dot{\psi} \\ \dot{\phi} \end{bmatrix}, \text{and } \mathbf{F}_R = \begin{bmatrix} F_X \\ F_Y \\ T_Z \\ T_\phi \end{bmatrix},$$

where M is the mass of a robot, I_z the moment of inertia about the *z*-axis passing through the robot center and I_ϕ the moment of inertia about the steering axis of the wheel modules. Note that the subscript R represents the fixed reference coordinate system.

The transformation matrix from the moving to the absolute coordinate system is given by

$$\mathbf{R}=\begin{bmatrix}\cos\psi & -\sin\psi & 0 & 0\\ \sin\psi & \cos\psi & 0 & 0\\ 0 & 0 & 1 & 0\\ 0 & 0 & 0 & 1\end{bmatrix} \quad (3)$$

The relationship between the fixed reference frame and the moving robot frame is described by

$$\mathbf{V}_R=\mathbf{R}\cdot\mathbf{V}_r,\quad \mathbf{F}_R=\mathbf{R}\cdot\mathbf{F}_r \quad (4)$$

Differentiation of $\mathbf{V}_R$ is given by

$$\dot{\mathbf{V}}_R=\mathbf{R}\dot{\mathbf{V}}_r+\dot{\mathbf{R}}\mathbf{V}_r \quad (5)$$

Therefore, the robot of Eq. (2) is described on the moving coordinate system by

$$\mathbf{M}_r(\mathbf{R}\dot{\mathbf{V}}_r+\dot{\mathbf{R}}\mathbf{V}_r)=\mathbf{R}\mathbf{F}_r \text{ or } \mathbf{R}^{-1}\mathbf{M}_r(\mathbf{R}\dot{\mathbf{V}}_r+\dot{\mathbf{R}}\mathbf{V}_r)=\mathbf{F}_r \quad (6)$$

The above equation neglected friction forces. If the friction force term is added to Eq. (6), the motion of the robot is described by

$$\mathbf{M}_r\dot{\mathbf{V}}_r+\mathbf{R}^{-1}\mathbf{M}_r\dot{\mathbf{R}}\mathbf{V}_r+\mathbf{f}_r=\mathbf{F}_r \quad (7)$$

where $\mathbf{f}_r$ represents the friction force and torque and it is described by

$$\mathbf{f}_r=\begin{bmatrix}f_x\,\mathrm{sgn}(v_x) & f_y\,\mathrm{sgn}(v_y) & \tau_\psi\,\mathrm{sgn}(\dot{\psi}) & \tau_\phi\,\mathrm{sgn}(\dot{\phi})\end{bmatrix}^T \quad (8)$$

On the other hand, the force and moment of a robot can be expressed from the geometry in Fig. 1 by

$$\mathbf{F}_r=\mathbf{J}^{-T}\mathbf{F}_w \text{ or } \mathbf{F}_w=\mathbf{J}^T\mathbf{F}_r \quad (9)$$

where $\mathbf{F}_w=[F_1\ F_2\ F_3\ F_4]^T$, $\mathbf{F}_r=[F_x\ F_y\ T_z\ T_\phi]^T$.

Here, $\mathbf{F}_x$ and $\mathbf{F}_y$ are the forces acting on the robot center in the x and y directions, T_z is the moment about the z axis passing through the robot center, and T_ϕ is the torque required to rotate the wheel modules, respectively. Note that the force F_i (i = 1,.., 4) is the traction force acting on the wheel in the direction of active rolling as shown in Fig. 2.

In addition, the wheel forces are given by

$$R\mathbf{F}_w=\mathbf{U}-I_w\dot{\boldsymbol{\omega}}_w-c_w\boldsymbol{\omega}_w \text{ or } R\mathbf{F}_w=\mathbf{U}-\frac{I_w}{R}\dot{\mathbf{V}}_w-\frac{c_w}{R}\mathbf{V}_w \quad (10)$$

where R is the wheel radius, $\mathbf{U}=[u_1\ u_2\ u_3\ u_4]^T$ where u_i is the motor torque generated by the i-th motor, I_w is the moment of inertia of the wheel about the wheel axis and c_w is the viscous friction factor of the wheel, and $\boldsymbol{\omega}_w=[\omega_1\ \omega_2\ \omega_3\ \omega_4]^T$ where ω_i is the angular velocity of the i-th wheel. From Eq. (1), the wheel velocity and acceleration vectors are obtained by

$$\mathbf{V}_w=\mathbf{J}^{-1}\mathbf{V}_r,\quad \dot{\mathbf{V}}_w=\dot{\mathbf{J}}^{-1}\mathbf{V}_r+\mathbf{J}^{-1}\dot{\mathbf{V}}_r \quad (11)$$

After substitution of Eq. (9), (10) and (11) into (7), the following relation is obtained by use of the relation

$$\mathbf{R}^{-1}\mathbf{M}_r\mathbf{R}=\mathbf{M}_r$$

$$\mathbf{U}=(R\mathbf{J}^T\mathbf{M}_r+\frac{I_w}{R}\mathbf{J}^{-1})\dot{\mathbf{V}}_r+(R\mathbf{J}^T\mathbf{R}^{-1}\mathbf{M}_r\dot{\mathbf{R}}+\frac{I_w}{R}\dot{\mathbf{J}}^{-1}+\frac{c_w}{R}\mathbf{J}^{-1})\mathbf{V}_r+R\mathbf{J}^T\mathbf{f}_r \quad (12)$$

Eq. (12) represents the dynamic model of a robot.

D. Velocity and Force Ratios

Since the omnidirectional mobile robot is of 3 DOFs in the 2-D plane, it is difficult to define the velocity ratio in terms of scalar velocities. Thus the velocity ratio is defined using the concept of norms as follows:

$$r_v=\frac{\|\mathbf{V}_r\|}{\|\mathbf{V}_w\|}=\frac{\|\mathbf{J}\mathbf{V}_w\|}{\|\mathbf{V}_w\|} \quad (13)$$

The force ratio of the force acting on the robot center to the wheel traction force can be defined in the same way as the velocity ratio in Eq. (13) as follows:

$$r_f=\frac{\|\mathbf{F}_r\|}{\|\mathbf{F}_w\|}=\frac{\|\mathbf{J}^{-T}\mathbf{F}_w\|}{\|\mathbf{F}_w\|} \quad (14)$$

Note that the force ratio corresponds to the inverse of the velocity ratio. Fig. 5 shows the force ratio profiles as a function of steering angle in the case of L_o = 0.283m, l = 0.19m, and θ = 45°. The translational force ratios vary significantly in the range between 0 and 2, while the rotational force ratio is kept nearly constant, when the steering angle is within the range between $-\phi_{\max}$ and $+\phi_{\max}$ ($0° < \phi_{\max} < 45°$). It is observed that the range of force ratio becomes wide as the steering angle grows in either sense.

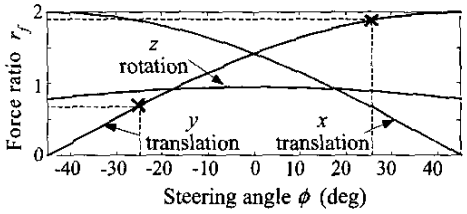

Fig. 5 Force ratio as a function of steering angle.

III. CONTROL OF CVT OF OMR-SOW

In this section, a control algorithm for the CVT is discussed. The CVT of an automobile can keep the engine running within the optimal range with respect to fuel efficiency or performance. Using the engine efficiency data, the CVT controls the engine operating points under various vehicle conditions. A CVT control algorithm for the OMR-SOW ought to include the effects of all four motors. A simple and effective algorithm for control of the CVT is proposed based on the analysis of the operating points of a motor.

A. Motion Control of OMR-SOW

The motion of a mobile robot can be controlled by wheel velocities. From Eq. (1), when the desired robot motion is given, the reference velocity of each wheel can be computed by

$$\mathbf{V}_{wref} = \mathbf{J}^{-1}\mathbf{V}_{rref} \tag{15}$$

If each wheel is controlled to follow the reference velocity, then the robot can achieve the desired motion. Practically, all mobile robots have slip between the wheels and the ground to some extent. This slip causes the real motion to be different from the desired one. If a steering angle is changed, a Jacobian of the OMR-SOW is also changed. Since the Jacobian affects all motions of a robot, the steering angle has to be controlled accurately. To measure a steering angle, an optical encoder is installed at the steering axis.

To compensate for a steering angle error, the reference steering velocity $\dot{\phi}_{ref}$ can be obtained by the difference between the reference steering angle ϕ_{ref} and the steering angle ϕ measured by the encoder as follows

$$\dot{\phi}_{ref} = K_{\phi}(\phi_{ref} - \phi) \tag{16}$$

where K_{ϕ} is the control gain of steering. The steering angle can follow the reference steering angle by proper control. Fig. 6 shows the control system with compensation for a steering angle.

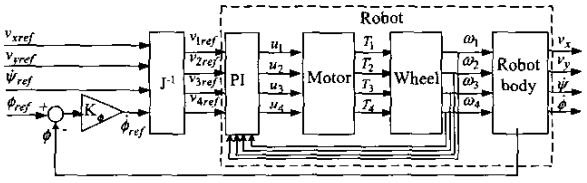

Fig. 6 Control structure of OMR-SOW.

B. Operating Points of a Motor

Fig. 7 shows operating points of a motor used in the mobile robot. In the figure T_{max} is the maximum continuous torque, ω_{max} is the maximum permissible angular velocity, the solid lines represent constant efficiency and the dashed lines denote constant output power. The input power is obtained by the product of input current and voltage and the output power is measured by the product of motor angular velocity and torque. The efficiency η is the ratio of the output to input power.

It is shown in this figure that the efficiency varies as the operating point moves on the constant output power line. The operating point of a motor is changed by a CVT. For the same output power, a reduction in the force ratio of a CVT leads to a decrease in velocity and an increase in torque and then a decrease in efficiency. It is desirable, therefore, that the CVT be controlled so that motors operate in the region of high velocity and low torque.

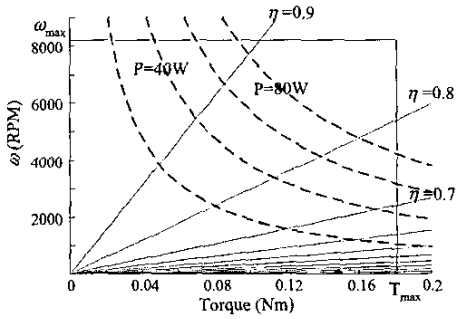

Fig. 7 Operating range of a motor.

C. Steering Algorithm

Given a reference input a robot is to follow, a steering algorithm for the OMR-SOW ought to determine the steering angle for efficient motor drive. The steering algorithm has to adapt to arbitrary reference inputs. Furthermore, it should be capable of adjusting steering angles smoothly for a smooth change in reference input.

The goal of a steering algorithm is to improve energy efficiency. For better efficiency, a higher force ratio is required so that a motor generates higher velocity and lower torque. If the desired force is obtained, the steering angle ought to be determined to maximize the force ratio for the obtained force.

In this thesis, two methods to obtain the desired force are proposed. One method is based on a dynamic model and the other uses information on the measured motor current. When the desired velocity is given as $\mathbf{V}_{rd}$ and a robot is controlled to follow it, the desired force can be obtained based on the dynamic model or the measured motor current. First, consider the method to use the dynamic model. If the dynamic model of Eq (7) is used, the desired force $\mathbf{F}_{rd}$ to follow the desired velocity can be directly obtained by

$$\mathbf{F}_{rd} = \mathbf{M}_r\dot{\mathbf{V}}_{rd} + \mathbf{R}^{-1}\mathbf{M}_r\dot{\mathbf{R}}\mathbf{V}_{rd} + \mathbf{f}_r \tag{17}$$

Next, consider the method to use measured motor currents. When a robot is controlled to track the reference trajectory, the motion controller provides the current to the motor required for the desired motion. Thus, if motor current is measured, the corresponding wheel traction force can be computed. If the measured motor current is substituted into Eq. (10), $\mathbf{F}_{wd}$ is given by

$$R\mathbf{F}_{wd} = \mathbf{U} - I_w\dot{\omega}_w - c_w\omega_w \tag{18}$$

From Eq. (9), the desired force $\mathbf{F}_{rd}$ is related to $\mathbf{F}_{wd}$ as follows

$$\mathbf{F}_{rd} = \mathbf{J}^{-T}\mathbf{F}_{wd} \tag{19}$$

Combining Eq. (18) and (19) yields

$$\mathbf{F}_{rd} = \mathbf{J}^{-T}(\mathbf{U} - I_w\dot{\omega}_w - c_w\omega_w)/R \tag{20}$$

In the method based on the dynamic model, if a reference trajectory is given, the desired force is easily obtained from Eq. (17). If there is a modeling error or

disturbance such as a ramp, however, this model cannot provide the real desired force. On the other hand, if the desired force is obtained from Eq. (20) using the measured current, disturbance can be reflected. That is, even when disturbance occurs, the robot moves to follow the same trajectory and the motor current is properly adjusted to reflect a change due to the disturbance. This fact is detailed in the experiments discussed in the next section.

Then, for the desired force of Eq. (17) and (20), the steering angle which maximizes the force ratio, is represented by

$$\phi_d = \arg(r_{f\max}(\mathbf{F}_{rd})) \tag{21}$$

In Eq. (9), the torque T_ϕ required to steer the wheel module is independent of steering angles. As shown in Fig. 5, the force ratio for rotation has little relation with steering angles. For this reason, the force ratio is governed mostly by translational motions. Let us define a force direction by translational motions as shown in Fig. 1.

$$\gamma_f = \text{angle}(F_{xd}, F_{yd}) \tag{22}$$

Fig. 8 shows the force ratio as a function of force direction and steering angle. When the force direction is given, a steering angle for the maximum force ratio can be found as a dashed line in Fig. 9. It is observed that the steering angle is not a continuous function of driving direction. For example, the steering angle is $-30°$ for the driving direction of $44.9°$, but $30°$ for the driving direction of $45.1°$. A jump in the steering angle due to a small change in driving direction is not desirable. For this reason, the steering angle is given as a function of driving direction such as a solid line in Fig. 9. This steering angle shows a smooth change for a smooth change in reference input and the force ratio profile is similar to the profile for the maximum force ratio.

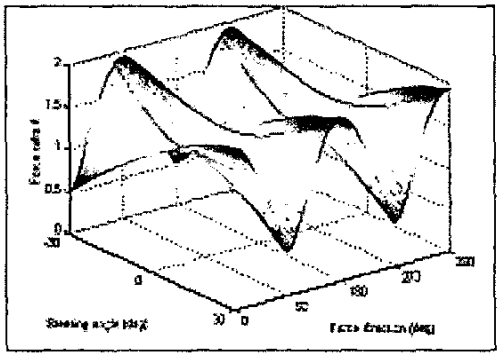

Fig. 8 Force ratio for steering angle and force direction

IV. EXPERIMENTS AND DISCUSSIONS

Various tests have been conducted to demonstrate performance of the constructed omnidirectional mobile robot with CVT function. A series of experiments using a fixed steering angle and a steering angle computed by the proposed algorithm have been conducted. In Fig. 10, the robot follows a 1.2m x 1.2m square trajectory at a speed of 0.05m/s. Fig. 10(a) shows the result using a fixed steering angle and the consumed energy is measured as 221.3J. In the experiments of (b), the steering angle is chosen by the force direction computed using a dynamic model. When the reference trajectory is given, the steering angle is chosen by Eq. (17) and Fig. 9. In case of (c), the steering angle is chosen by the force direction computed using measured currents by Eq. (20) and Fig. 9. The energy values for these experiments are measured, respectively, as 178.2J and 179.5J. For the same reference trajectory, the proposed two algorithms have a similar steering angle. It is shown that the consumed energies are reduced 15% by the proposed steering algorithms.

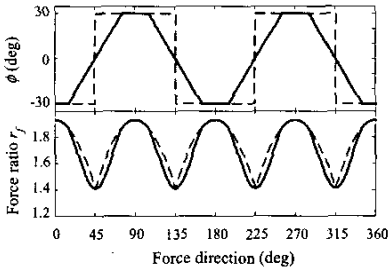

Fig. 9 Steering angle and force ratio for force direction

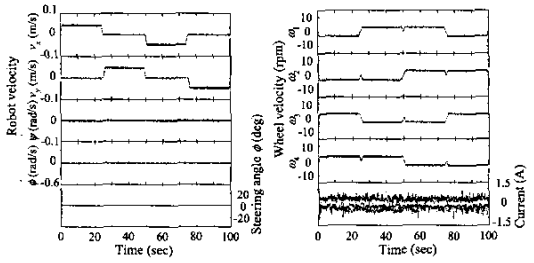

(a) Fixed steering angle

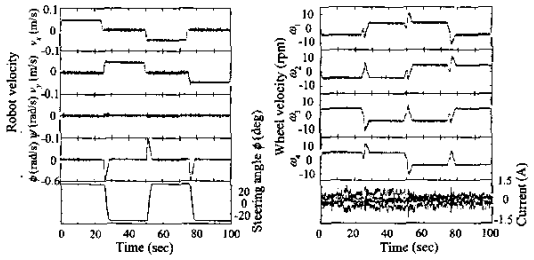

(b) Steering algorithm based on dynamic model

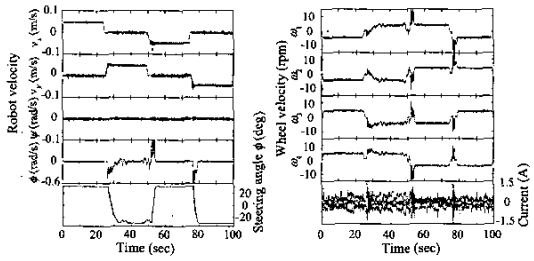

(c) Steering algorithm based on measured currents

Fig. 10 Experimental results for square trajectory

Experimental results for a square trajectory with 10° ramp shown in Fig. 11 are illustrated in Fig. 12. Fig. 12(a) shows the result using a fixed steering angle. When the robot climbs up the ramp, the current increases. The consumed energy is 765.7J. Fig. 12(b) shows the experimental results using the steering algorithm based on the dynamic model of a robot. This dynamic model does not include the ground conditions (e.g., a ramp) and disturbance (e.g., load change). Although a ramp exists on the path, the steering algorithm chooses the steering angle only based on the reference trajectory. The consumed energy is then increased 20% and measured as 932.4J. To overcome this problem, the dynamic model should reflect the ground condition. If a sensor (e.g., inclinometer) to measure the ground condition is installed, it can be included in the dynamic model of the robot. On the other hand, Fig. 12(c) shows the result using the steering algorithm based on the measured currents. If there is a ramp or disturbance, currents are changed to follow the desired motion of a robot. The measured currents indirectly include information about the condition of ground or disturbance. Even for a ramp or disturbance, therefore, the steering algorithm based on the measured current chooses proper steering angles. The consumed energy is reduced 14% and measured as 653.4J.

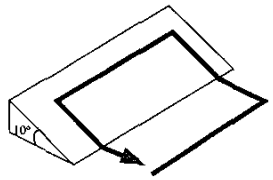

Fig. 11 Trajectory with ramp

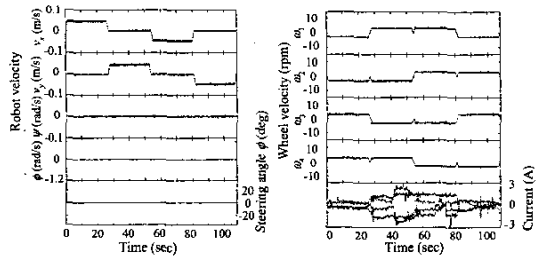

(a) Fixed steering angle

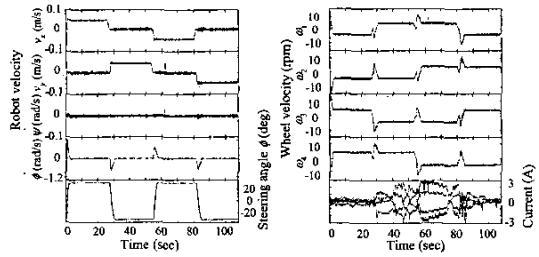

(b) Steering algorithm based on dynamic model

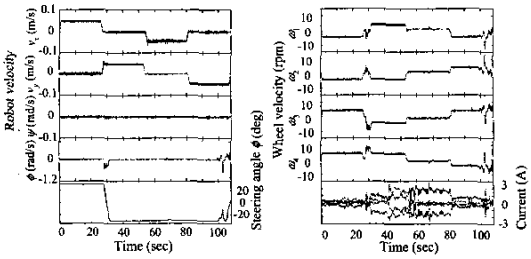

(c) Steering algorithm based on measured currents

Fig. 12 Experimental results for square trajectory with ramp

V. CONCLUSIONS

In this research, a steering algorithm for CVT of the OMR-SOW has been proposed. Since the motor efficiency is high in the region of high velocity and low torque, it controls a steering angle so that motors may operate in this region. The proposed algorithm calculates the steering angle to maximize the force ratio for a given force direction. The force direction is obtained by two methods; one is based on the dynamic model and the other on the measured motor current. Experimental results show that the proposed algorithm for CVT is more energy efficient than the one using a fixed steering angle.

VI. REFERENCES

[1] J. F. Blumrich, "Omnidirectional vehicle," *United States Patent* 3,789,947, 1974.

[2] B. E. Ilou, "Wheels for a course stable self-propelling vehicle movable in any desired direction on the ground or some other base," *United States Patent* 3,876,255, 1975.

[3] M. West and H. Asada, "Design of ball wheel mechanisms for omnidirectional vehicles with full mobility and invariant kinematics," *Journal of mechanical design*, Vol. 119, pp.153-161, 1997.

[4] M. Wada and S. Mory, "Holonomic and omnidirectional vehicle with conventional tires," *Proc. of ICRA*, pp. 3671-3676, 1996.

[5] K.-S. Byun, S.-J. Kim and J.-B. Song, "Design of a Four-Wheeled Omnidirectional Mobile Robot with Variable Wheel Arrangement Mechanism," *Proc. of ICRA*, pp.720-725, 2002.

[6] M. Wada and H. Asada, "Design and control of a variable footprint mechanism for holonomic omnidirectional vehicles and its application to wheelchairs," *IEEE Transactions on Robotics and Automation*, Vol. 15, No. 6, pp. 978-989, 1999.

[7] S. Liu and B. Paden, "A survey of today's CVT controls," *Proc. of the 36th conference on decision & control*, pp. 4738-4743, 1997.

[8] Z. Zou and Y. Zhang, "Ratio control of traction drive continuously variable transmissions," *Proc. of American Control Conference*, pp. 1525-1529, 2000.

[9] K.-S. Byun, S.-J. Kim and J.-B. Song, "Design of continuous alternate wheels for omnidirectional mobile robots," *Proc. of ICRA*, pp. 767-772, 2001.